Pulsed optically pumped frequency standard

Aldo Godone, Salvatore Micalizio, and Filippo Levi
Istituto Elettrotecnico Nazionale Galileo Ferraris, Strada delle Cacce 91, 10135 Torino, Italy
(Received 18 December 2003; revised manuscript received 20 April 2004; published 19 August 2004)

We reconsider the idea of a pulsed optically pumped frequency standard conceived in the early 1960s to eliminate the light-shift effect. The development of semiconductor lasers and of pulsed electronic techniques for atomic fountains and new theoretical findings allow an implementation of this idea which may lead to a frequency standard whose frequency stability is limited only by the thermal noise in the short term and by the temperature drift in the long term. We shall also show both theoretically and experimentally the possibility of doubling the atomic quality factor with respect to the classical Ramsey technique approach.

DOI: 10.1103/PhysRevA.70.023409 PACS number(s): 32.80.Bx, 06.30.Ft, 32.30.Bv

I. INTRODUCTION

An increasing demand is observed for local oscillators with high-frequency stability in the short and medium term in different application fields such as radionavigation, telecommunication, and high-resolution spectroscopy. Strong efforts are then devoted to the development, among others, of optically pumped frequency standards based on cells containing vapors of alkali-metal atoms (^{87}Rb, ^{133}Cs) due to their simple physical operation, compactness, and reliability [1]. In this framework, we intend to reconsider the idea of pulsed optical pumping originally conceived by Alley [2] in 1960 and first applied to the field of frequency standards by Arditi and Carver [3] in 1964. The development of semiconductor lasers and of pulsed electronics for atomic fountains together with new theoretical results allows a very promising implementation of this idea that we examine in this paper both theoretically and experimentally.

Before discussing in more detail the expected behavior of a pulsed optically pumped (POP) frequency standard we discuss the main reasons this reproposal is based on.

In the rf-optical double-resonance approach of the traditional vapor cell frequency standards [4], the lamp or laser instabilities are transferred to the clock signal due to the simultaneous presence in time and in space of the optical pumping, interrogation, and detection phases. In this case, in fact, the atomic sample operates as a three-level system and the coupling of the microwave and optical coherences leads to various physical effects such as light shift, power shift, etc., which impair the theoretical shot noise limit [5]. A partial reduction of those problems has been achieved using the more symmetrical Λ excitation scheme: the microwave clock transition is observed through the electromagnetically induced transparency (EIT) signal [6] or through the emission profile of the coherent population trapping (CPT) maser [7,8]. In this more recent class of passive oscillators the physical effects which impair the frequency stability may be compensated and/or reduced but not fully eliminated. In particular, it has been theoretically shown that the use of a frequency-modulated laser spectrum with a proper modulation index may lead to a cancellation of the amplitude or frequency light shift [9]; the effectiveness of this technique has been experimentally demonstrated even if a full compensation may require a severe control of the modulation index.

In the POP operation the pumping, interrogation, and detection phases are separated in time in such a way that during the clock interrogation the atomic sample behaves as a pure two-level system avoiding the coupling between microwave and optical coherences. We shall consider in particular the case of pulsed optical pumping performed by a semiconductor laser on a cell containing buffer gas, separated in time by a Ramsey interaction scheme defined by a double microwave pulse; the transition signal is then detected through the free-induction decay observed via a high-Q microwave cavity at the end of the second Ramsey pulse. This technique avoids in principle the light-shift effect [10] and the noise conversions from the laser to the clock signal. The microwave detection allows us to reach the thermal noise limit without any laser background signal and to obtain a higher atomic quality factor Q_a due to the direct detection of the induced microwave coherence instead of the population inversion. In fact, when the atoms are submitted to $\pi/2$ Ramsey pulses, the component of the Bloch vector related to the microwave coherence rotates at a double speed with respect to the component related to the population inversion, as will be discussed and proved in the paper. Finally, we shall also report an evaluation of the short- and medium-term frequency stability achievable in the case of a practical experimental setup.

II. THEORY

In this section we shall report first the basic equations which describe the behavior of an optically pumped frequency standard, taking into account tha cavity feedback and the optical thickness of the atomic medium. The following step aims to find the physical operating conditions required to uncouple the optical pumping and the microwave interrogation process in order to avoid any time overlap between the optical and microwave coherences.

In the last step we shall derive the theoretical expressions describing the Ramsey pattern as observed through the optical transmitted signal or the free-induction decay signal at the cavity output.

The theory developed in the following considers the schematic setup shown in Fig. 1. The atomic medium is a low-pressure vapor of ^{87}Rb contained in a quartz cell of length L

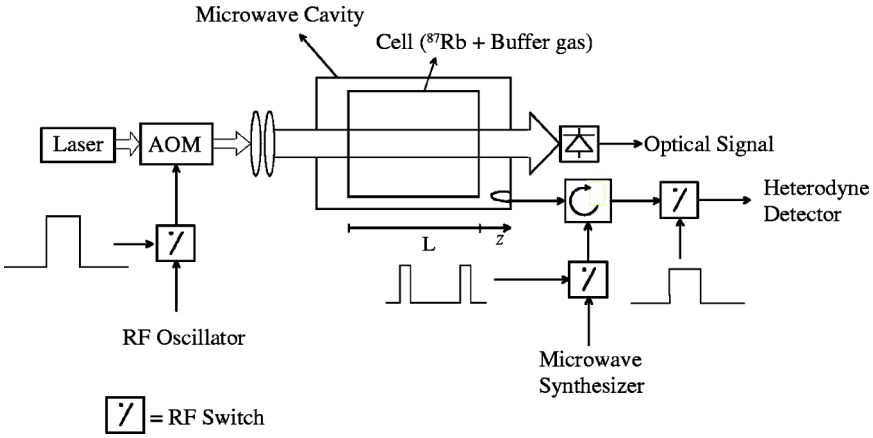

FIG. 1. Schematic setup of the POP frequency standard. AOM: acousto-optic modulator.

with buffer gas placed in a microwave cavity operating in the TE_{011} mode and tuned to the ground state hyperfine transition frequency. In the following we consider that the ^{87}Rb atoms are optically pumped through a pulsed laser light tuned to the D_1 transition even if the theory here developed holds for other alkali metals and for the D_2 optical transition. The atomic levels involved in the POP operation are shown in Fig. 2 where γ_1 and γ_2 are the relaxation rates of the population difference and of the coherence of the ground-state hyperfine levels, Γ^* is the decay rate of the state $|m\rangle$, and Δ_0 is the laser detuning with respect to the optical transition. The static quantization magnetic field is applied along the z direction. The relaxation rates γ_1, γ_2, and Γ^* take into account the interaction of the atomic vapor with the buffer gas [4]; due to such an interaction, the atoms are localized with respect to the wavelength of the microwave field. The POP timing sequence, generated by the three electronic switches (shown in Fig. 1), is indicated in Fig. 3 together with the characteristic times involved in the operation. In Fig. 3, ω_R is the optical Rabi frequency at the entrance of the cell and b_e the Rabi frequency related to the external microwave signal applied to the cavity. A theoretical approach of the POP system is reported in Ref. [11]; here we follow a more complete theory developed in Ref. [12] for the CPT frequency standards where the effect of the microwave cavity is taken into account.

In the formalism of the ensemble-averaged density matrix and in the rotating-wave approximation the following set of equations holds:

$$\dot{\Delta} + \left(\gamma_1 + \frac{\Gamma_p}{1+\delta_0^2}\right)\Delta = -2b_e \mathrm{Im}(e^{-i\phi_e}\delta_{\mu\mu'}) - 2\mathrm{Im}(\tilde{b}_i^*\delta_{\mu\mu'}) + \frac{\Gamma_p}{1+\delta_0^2},$$

$$\dot{\delta}_{\mu\mu'} + \left[\gamma_2 + \frac{\Gamma_p}{1+\delta_0^2} + i\left(\Omega_\mu + \frac{\Gamma_p\delta_0}{1+\delta_0^2}\right)\right]\delta_{\mu\mu'} = i\frac{b_e}{2}e^{i\phi_e}\Delta + i\frac{\tilde{b}_i}{2}\Delta,$$

$$\frac{\partial\omega_R}{\partial z} + \frac{1}{c}\frac{\partial\omega_R}{\partial t} = -\alpha\frac{\omega_R}{2\Gamma^*}\frac{1-\Delta}{1+\delta_0^2},$$

$$\tilde{b}_i(t) = -2ike^{i\psi}\frac{1}{L}\int_0^L \delta_{\mu\mu'}(z,t)dz,$$

$$\rho_{mm} = \frac{\Gamma_p}{\Gamma^*}\frac{1-\Delta}{1+\delta_0^2}. \quad (1)$$

In system (1), $\Delta = \rho_{\mu'\mu'} - \rho_{\mu\mu}$ is the ground-state population difference, $\delta_0 = 2\Delta_0/\Gamma^*$ is the normalized laser detuning, $\Gamma_p = \omega_R^2/2\Gamma^*$ is the longitudinal pumping rate, ϕ_e is an arbitrary phase reference for the external microwave Rabi frequency b_e, $\tilde{b}_i$ is the complex Rabi frequency associated with the microwave field generated by the atomic ensemble, $\Omega_\mu = \omega_0 - \omega_{\mu\mu'}$ is the microwave detuning, c is the speed of light in vacuum, and α the linear absorption coefficient of the optical radiation. Moreover, $\delta_{\mu\mu'}$ is the slowly varying part of the hyperfine coherence, ψ and k are the cavity detuning parameter and the number of microwave photons emitted by an atom in 1 s, as defined in Ref. [8]:

$$k = \frac{\mu_0\mu_B^2\eta' Q_L n}{\hbar(2I+1)},$$

$$\psi = 2Q_L\frac{\Delta\omega_c}{\omega_{\mu\mu'}}, \quad (2)$$

where μ_0 is the vacuum permeability, μ_B is the Bohr magneton, η' is the cavity filling factor defined in Ref. [7], Q_L is the loaded cavity quality factor, I is the nuclear spin, n is the atomic density, and $\Delta\omega_c$ is the cavity detuning from $\omega_{\mu\mu'}$. In Eq. (1), $\Delta, \delta_{\mu\mu'}$, and $\omega_R(\Gamma_p)$ are functions of z and t in the most general case. The system has been derived in the limit of the adiabatic approximation for the optical coherences ($\dot{\delta}_{\mu m} = \dot{\delta}_{\mu' m} = 0$) and under the following hypotheses well satisfied in our experimental conditions:

$$\omega_R(z,t) \ll \Gamma^* \quad \text{for each } z \text{ and } t,$$

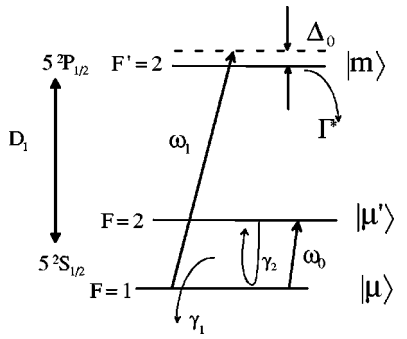

FIG. 2. Three-level system considered in the text.

$$\Omega_\mu \ll \Gamma^*, \qquad b_e \ll \Gamma^*. \tag{3}$$

In this formalism the optical transmitted signal is proportional to $\omega_R^2(z=L)$, the fluorescence signal at z is proportional to $\rho_{mm}(z)$, and the free-induction decay at the cavity output after the microwave excitation is [7,8]

$$P_a(t) = \frac{1}{2}\hbar\omega_{\mu\mu'}N_a\frac{|\tilde{b}_i(t)|^2}{k}, \tag{4}$$

where N_a is the number of atoms in the effective volume V_a of the cell exposed to the laser field $[N_a = nV_a/(2I+1)]$.

When the timing sequence of Fig. 3 is periodic, with period T_c, it is important to avoid any time overlap between the optical and microwave coherences in order to uncouple the interrogation and the optical pumping phases as discussed in Sec. I. The decay rate of the optical coherence is very fast, of the order of Γ^*, while the decay rate of the hyperfine coherence may be as slow as γ_2. In order to avoid long dead times in the POP operation, the laser pulse must ensure not only a sufficient population inversion between the two ground-state levels but also a strong reduction of the residual microwave coherence between one cycle and another. Having this goal in mind, we evaluate the required intensity and duration of the laser pulse in the following way: in the optical pumping phase $b_e=0$ and the feedback of the cavity on the atomic system may be neglected ($k\sim 0$), so that system (1) simplifies as follows:

$$\dot{\Delta} + (\gamma_1 + \Gamma_p)\Delta = \Gamma_p,$$

$$\dot{\delta}_{\mu\mu'} + [\gamma_2 + \Gamma_p + i(\Omega_\mu + \Gamma_p\delta_0)]\delta_{\mu\mu'} = 0,$$

$$\frac{\partial\Gamma_p}{\partial z} = -\frac{\alpha}{\Gamma^*}\Gamma_p(1-\Delta), \tag{5}$$

where we have assumed $\delta_0 \ll 1$. In our typical experimental situation $\partial\Gamma_p/(c\,\partial t) \ll \partial\Gamma_p/\partial z$ and has been omitted in Eqs. (5). The solution of the second differential equation is straightforward:

$$\delta_{\mu\mu'}(z,t_p) = \delta_{\mu\mu'}(z,0^+)e^{-(\gamma_2+\Gamma_p)t_p}e^{i(\Omega_\mu+\Gamma_p\delta_0)t_p} \quad \text{for each } z, \tag{6}$$

$t=0^+$ being the beginning of the laser pulse and t_p its duration.

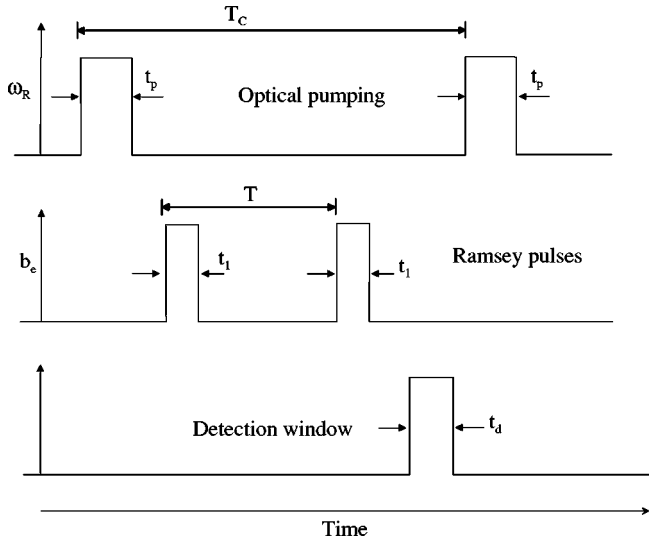

FIG. 3. POP timing sequence: T_c, cycle period; t_p, optical pumping time; t_1, Rabi time; T, Ramsey time; t_d, detection time.

From Eq. (6) it turns out that a residual microwave coherence at $t=0^+$ is reduced by the laser pulse by a factor $e^{-\Gamma_p t_p}$ and the same holds for the light-shift contribution $\Gamma_p\delta_0$ present in the rotating term. The following condition must then be satisfied:

$$\Gamma_p(z)t_p \gg 1 \quad \text{for all } z. \tag{7}$$

Due to the absorption of the atomic medium, $\Gamma_p(z)$ is a decreasing function of z, so that the condition (7) implies

$$\Gamma_p(L)t_p \gg 1. \tag{8}$$

The first and third equations of system (5) in steady-state conditions give

$$\ln\frac{\Gamma_p(L)}{\Gamma_p(0)} + \frac{1}{\gamma_1}[\Gamma_p(L) - \Gamma_p(0)] = -\zeta, \tag{9}$$

where $\zeta = \alpha L/\Gamma^*$ is the optical length of the cell. In the typical case of interest, $\zeta > 1$, the logarithmic term in Eq. (9) can be omitted so that the condition (8) becomes

$$\Gamma_p(0) \gg \zeta\gamma_1 + \frac{1}{t_p}. \tag{10}$$

Under this condition the optical pumping and the interrogation phases are really separated and the atomic sample behaves as a two-level system in both phases.

The atom-microwave interaction during the first Ramsey pulse is described by the simplified system of equations:

$$\dot{\Delta} = 2b_e\mathrm{Re}\,\delta_{\mu\mu'},$$

$$\dot{\delta}_{\mu\mu'} = -i\Omega_\mu\delta_{\mu\mu'} - \frac{b_e}{2}\Delta, \tag{11}$$

which has been obtained by Eq. (1) (with $\phi_e = \pi/2$) taking into account the following.

(i) In this phase the laser is off ($\Gamma_p=0$).

(ii) $t_1 \ll \gamma_1^{-1}$ and $t_1 \ll \gamma_2^{-1}$ so that the decay rates may be neglected during the microwave pulse.

(iii) The feedback of the cavity on the atoms is negligible ($b_e \gg |\tilde{b}_i|$).

The solution of system (11) can be written in the compact form [4]

$$R(t) = M_I(t) \times R(0), \tag{12}$$

where $R(t)$ is the Bloch vector defined as

$$R(t) = \begin{pmatrix} \mathrm{Re}\,\delta_{\mu\mu'}(t) \\ \mathrm{Im}\,\delta_{\mu\mu'}(t) \\ \Delta(t) \end{pmatrix}. \tag{13}$$

Here $R(0)$ is the Bloch vector at $t=0$ (beginning of the microwave pulse) and $M_I(t)$ is the interaction matrix ($\xi^2 = b_e^2 + \Omega_\mu^2$):

$$M_I(t) = \begin{pmatrix} \cos \xi t & \frac{\Omega_\mu}{\xi} \sin \xi t & -\frac{b_e}{2\xi} \sin \xi t \\ -\frac{\Omega_\mu}{\xi} \sin \xi t & \frac{1}{\xi^2}(b_e^2 + \Omega_\mu^2 \cos \xi t) & \frac{\Omega_\mu b_e}{2\xi^2}(1 - \cos \xi t) \\ \frac{2b_e}{\xi} \sin \xi t & \frac{2\Omega_\mu b_e}{\xi^2}(1 - \cos \xi t) & \frac{1}{\xi^2}(\Omega_\mu^2 + b_e^2 \cos \xi t) \end{pmatrix}. \tag{14}$$

The free decay region between the two microwave pulses is described by the following system obtained from Eqs. (1) with $\omega_R = 0$ and $b_e = 0$:

$$\dot{\Delta} + \gamma_1 \Delta = -2\mathrm{Im}\left(\tilde{b}_i^* \delta_{\mu\mu'}\right),$$

$$\dot{\delta}_{\mu\mu'} + (\gamma_2 + i\Omega_\mu)\delta_{\mu\mu'} = i\frac{\tilde{b}_i}{2}\Delta,$$

$$\tilde{b}_i(t) = -2ike^{i\psi}\frac{1}{L}\int_0^L \delta_{\mu\mu'}(z,t)dz = -2ike^{i\psi}\delta_{\mu\mu'}. \tag{15}$$

In the last equation we disregard the space dependence of $\delta_{\mu\mu'}$ because a full optical pumping has been assumed at each z via Eq. (10).

In the practical case $\psi \ll 1$ and the system (15) then becomes

$$\dot{\Delta} + \gamma_1 \Delta = -4k|\delta_{\mu\mu'}|^2,$$

$$\dot{\delta}_{\mu\mu'} + (\gamma_2 + i\Omega_\mu)\delta_{\mu\mu'} = k(1 + i\psi)\Delta\,\delta_{\mu\mu'}. \tag{16}$$

At the moment we neglect the cavity feedback on the atoms ($k \ll \gamma_2$) mainly responsible for the cavity-pulling effect that we shall consider later on; in this case the solution of system (16) is given by the following decay matrix $M_D(t)$:

$$M_D(t) = \begin{pmatrix} e^{-\gamma_2 t}\cos \Omega_\mu t & e^{-\gamma_2 t}\sin \Omega_\mu t & 0 \\ -e^{-\gamma_2 t}\sin \Omega_\mu t & e^{-\gamma_2 t}\cos \Omega_\mu t & 0 \\ 0 & 0 & e^{-\gamma_1 t} \end{pmatrix}. \tag{17}$$

The Ramsey interaction is then simply described by the following matrix product:

$$R(t_0) = M_I(t_1) \times M_D(T) \times M_I(t_1) \times R(0), \tag{18}$$

where $t=0$ corresponds to the beginning of the first pulse and t_0 to the end of the second pulse. In Figs. 4 and 5, Ramsey patterns are reported as obtained from Eq. (18) when $R(0) = (0,0,1)$ for the optical signal (a) and for the free-induced decay signal (b) at the end of the second microwave pulse.

In Fig. 4, $\theta = \xi t_1 = \pi/8$, while in Fig. 5, $\theta = \pi/2$; in the second case the central Ramsey fringes observed through the free-induced decay show an oscillation period doubled with respect to the optical signal which leads to a doubled atomic quality factor Q_a. This is the main reason why we choose to detect the hyperfine transition through the microwave signal instead of the more common optical transmitted signal. This very interesting feature may be easily derived from the analytic expressions describing the central Ramsey fringe; in fact, developing Eq. (18) with $\Omega_\mu = 0$ only in the interaction matrix and with $\theta = \pi/2$ we obtain, when $t_1 \ll T$,

$$\Delta = -e^{-\gamma_2 T}\cos \Omega_\mu T,$$

$$|\delta_{\mu\mu'}|^2 = \frac{1}{4}e^{-2\gamma_2 T}\sin^2 \Omega_\mu T, \tag{19}$$

and for the corresponding full widths at half maximum,

$$\Delta\omega_{1/2} = \pi/T \quad \text{optical detection},$$

$$\Delta\omega_{1/2} = \pi/2T \quad \text{microwave detection}. \tag{20}$$

A physical interpretation of this behavior may be readily given in terms of Bloch's vectors. In fact, it is well known that any magnetic resonance experiment involving a two-level atom can be interpreted as a rotating fictitious 1/2 spin [13]. In particular, in our case the system is described by the equation [see Eq. (11)]

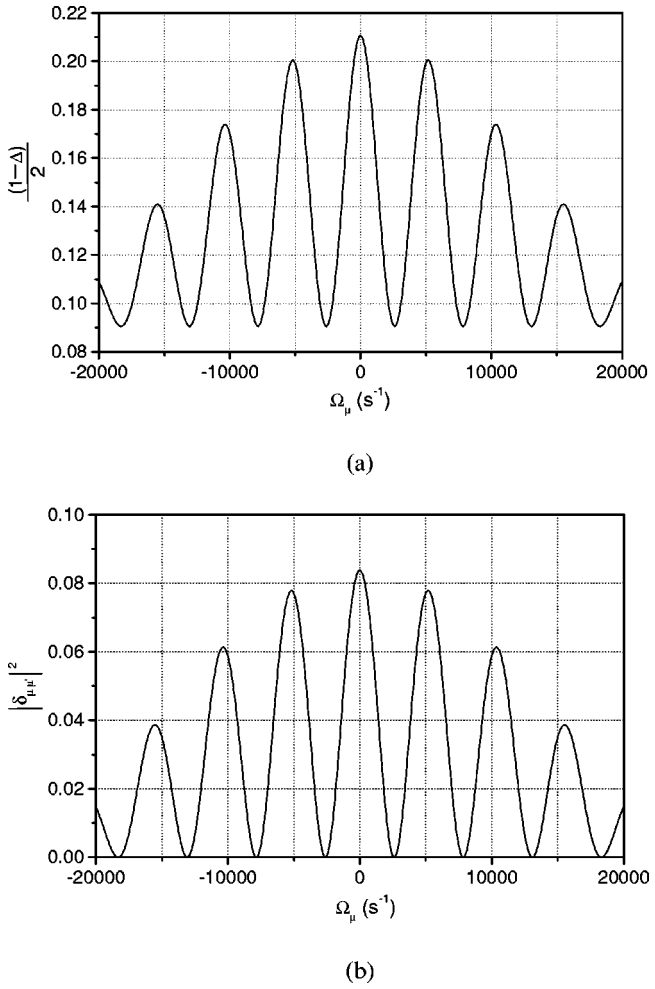

FIG. 4. Computed fringes corresponding to $\gamma_1=\gamma_2=200\ \mathrm{s}^{-1}, \Delta_0=0, t_1=200\ \mu\mathrm{s}, T=1$ ms, and $\theta=\pi/8$. (a) Optical signal and (b) free-induced decay signal.

$$\frac{d}{dt}\vec{r}(t)=\vec{r}(t)\wedge\vec{B}, \tag{21}$$

where the $\vec{r}(t)$ and $\vec{B}$ are defined in Eq. (22) and shown in Fig. 6:

$$\vec{r}(t)=\begin{pmatrix}2\mathrm{Re}\,\delta_{\mu\mu'}(t)\\ 2\mathrm{Im}\,\delta_{\mu\mu'}(t)\\ \Delta(t)\end{pmatrix},\quad \vec{B}=\begin{pmatrix}0\\ b_e\\ \Omega_\mu\end{pmatrix}. \tag{22}$$

To write Eq. (21) we neglect the decays of the coherence and of the population inversion also in the free evolution phase, since they introduce only a damping factor without affecting the main physical behavior of the atomic system.

Figure 7 shows the evolution of the fictitious spin submitted to the Ramsey interaction scheme for $\theta=\pi/2$ and for different microwave detunings. We suppose that the laser pulse performs a complete inversion of the ground-state population, so that at the initial instant $\vec{r}=(0,0,1)$. During the first Ramsey pulse, the effective magnetic field is directed along the y axis, assuming the condition $|\Omega_\mu|\ll b_e$, well satisfied for the central fringe of the Ramsey pattern. The spin then rotates around the y axis with a rotation angle of $\theta=\pi/2$. In the free evolution phase, $b_e=0$ and the spin processes around the z axis which supports the effective magnetic field equal to Ω_μ. The rotation angle is $\Omega_\mu T$, where T is, as usual, the Ramsey time. During the second Ramsey pulse, the spin makes again a rotation of $\theta=\pi/2$ around the y axis. From column (c) of Fig. 7 it is possible to observe that while the population (projection of the Bloch vector on the z axis) evolves from -1 to 1, half a cycle, the coherence (projection on the x-y plane) has already performed an entire cycle, evolving from 0 to its maximum value to 0 again. This behavior is fully described by Eqs. (19) which express the central Ramsey fringe of Δ and $|\delta_{\mu\mu'}|^2$, respectively. Therefore, for $\pi/2$ pulses, the free-induced decay signal ($\propto|\delta_{\mu\mu'}|^2$) shows an atomic quality factor that is twice that observed in the optical signal ($\propto\Delta$).

Relations (19) and (20) give the line shape and width of the response of the POP atomic system when Eq. (10) is satisfied; in this ideal case the atomic response is fully uncoupled from the laser parameters and no laser noise contribution is transferred to the microwave output signal. In practice a residual light-shift effect will still remain due to the finite laser intensity as well as a cavity pulling effect due to the feedback of the microwave cavity on the atomic sample, disregarded in the derivation of Eq. (17). We shall evaluate both these effects in the following sections.

III. RESIDUAL LIGHT SHIFT

It is clear from Eq. (6) that the laser pulse strongly destroys any residual hyperfine coherence before a new cycle starts up, avoiding in this way any "phase memory" [11] among consecutive cycles, and then the light shift. This ideal condition is reached in the limit of an arbitrary large laser intensity; in practice a residual light shift remains depending on how strongly the inequality (10) is satisfied.

The central Ramsey fringe, observed for example in the population difference $\Delta(\Omega_\mu)$, obtained from Eq. (18) for $\theta=\pi/2$ and with general initial conditions, is given by

$$\Delta(\Omega_\mu)_{t=T}=e^{-\gamma_2 T}\{2\mathrm{Im}\,\delta_{\mu\mu'}(0)\sin\Omega_\mu T-\Delta(0)\cos\Omega_\mu T\}, \tag{23}$$

whose maximum is shifted from the hyperfine frequency of

$$\frac{\Delta\omega}{\omega_{\mu\mu'}}=-\frac{1}{\pi Q_a}\arctan\frac{2\mathrm{Im}\,\delta_{\mu\mu'}(0)}{\Delta(0)}, \tag{24}$$

where $Q_a=\omega_{\mu\mu'}/\Delta\omega_{1/2}$ is the quality factor of the central Ramsey fringe. When the inequality (10) is satisfied we have $\mathrm{Im}\,\delta_{\mu\mu'}(0)\ll 1$ and $\Delta(0)\sim 1$ so that Eq. (24) gives

$$\frac{\Delta\omega}{\omega_{\mu\mu'}}=-\frac{2}{\pi Q_a}\mathrm{Im}\,\delta_{\mu\mu'}(0). \tag{25}$$

Equation (25) gives the expected residual light shift in terms of the residual coherence at the beginning of the first Ramsey pulse of a generic cycle. By solving Eqs. (6) and (18) with a recursive numerical approach, we evaluate the residual light shift in practical experimental conditions as reported in Figs.

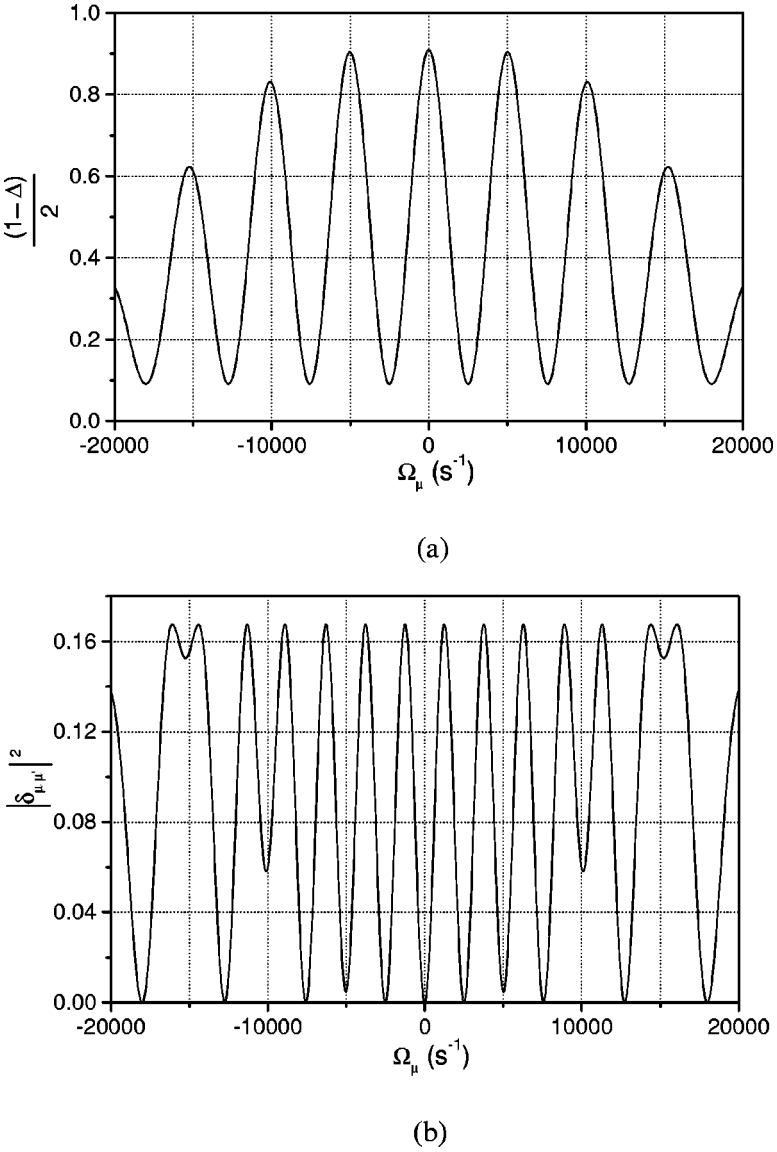

FIG. 5. Computed Ramsey fringes. Same parameters as in Fig. 4 but $\theta=\pi/2$.

8 and 9. The absolute frequency shift of the central Ramsey fringe is shown in Fig. 8 versus the laser detuning $\Delta_0/2\pi$, while the frequency shift versus the microwave pulse area $\theta=b_e t_1$ is reported in Fig. 9 for two different laser pumping rates.

When the laser intensity is increased, the reduction of the shift is evident as expected from Eqs. (6) and (25); moreover, for $\theta\sim\pi/2$ the residual light shift may be fully eliminated. The POP approach is free of the light-shift effect at a very high degree if compared with the rf and optical pumping approach and then no conversion of the laser noise into the microwave signal has to be expected provided inequality (10) is satisfied and $\pi/2$ pulses are used.

IV. CAVITY PULLING

The cavity-pulling effect is due to the feedback of the microwave cavity on the atomic sample mainly during the free decay time T between the two Ramsey pulses. In fact during that time the atoms are perturbed only by the electromagnetic field excited in the cavity by the hyperfine coherence whose decay time constant γ_2^{-1} is of the same order of magnitude of T.

A cavity detuning $\Delta\omega_c$ induces a dephasing in the free time evolution of the coherence $\delta_{\mu\mu'}$ which leads to a shift of the observed central Ramsey fringe from the hyperfine transition frequency. To evaluate the cavity pulling effect in Eq. (18), we must use the decay matrix $M_D(T)$ obtained by the solution of Eq. (16) without neglecting the coupling terms.

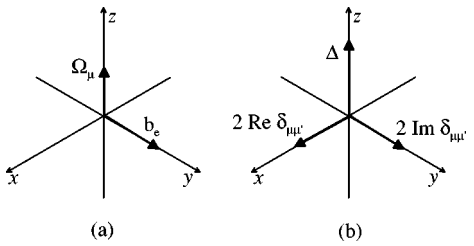

FIG. 6. (a) Components of the effective magnetic field and (b) components of the fictitious spin.

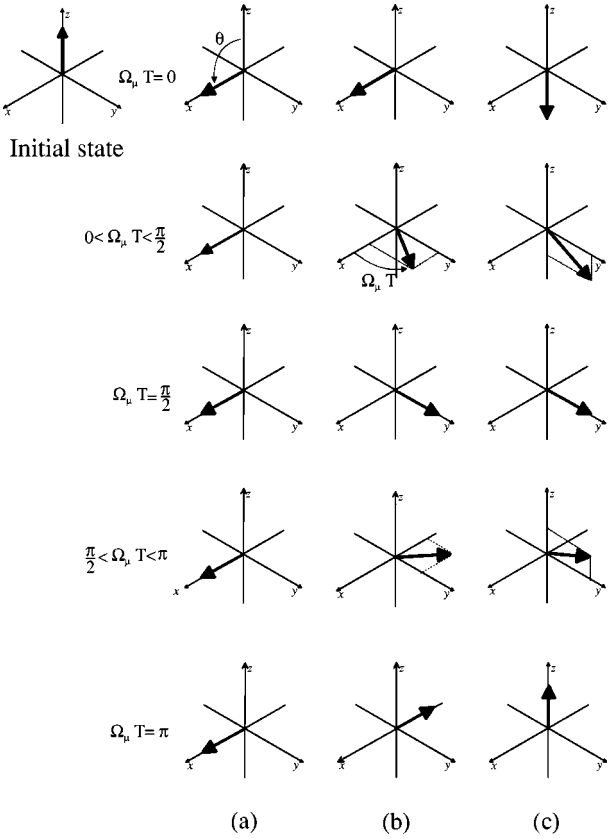

FIG. 7. Ramsey interaction in terms of fictitious spin for $\theta=\pi/2$ and for different microwave detunings Ω_μ. (a) First Ramsey pulse (rotation of θ around y axis), (b) free evolution phase (rotation of $\Omega_\mu T$ around z axis), and (c) second Ramsey pulse (rotation of θ around y axis). The first row corresponds to the resonance ($\Omega_\mu=0$) and the spin does not rotate during the free evolution phase. Column (c) gives the state of the atomic system after the second Ramsey pulse. While Δ (projection on the z axis) evolves from -1 to 1, the absolute value of the coherence (projection on the x-y plane) performs a complete cycle, starting from 0, for $\Omega_\mu=0$, and reaching its maximum for $\Omega_\mu T=\pi/2$ where $\Delta=0$.

The following analytical solution may be found for the cavity pulling of the central Ramsey fringe (see the Appendix):

$$\Delta\omega=-\frac{\psi}{T}\ln\left\{\cosh\left[\frac{k}{\gamma}(1-e^{-\gamma T})\right]+\cos\theta\sinh\left[\frac{k}{\gamma}(1-e^{-\gamma T})\right]\right\}, \tag{26}$$

where $\gamma=\gamma_1\sim\gamma_2$ is a condition typical for the alkali-metal vapors in buffer gas at the usual operating temperatures. A numerical evaluation of Eq. (26) is reported in Fig. 10 where the cavity-pulling shift is shown versus γT for different values of the parameter $k'=k/\gamma$ and for $\theta=\pi/2$.

When $\gamma T\gg 1, \Delta\omega\propto T^{-1}\propto Q_a^{-1}$, this behavior is well known in the field of atomic frequency standards [4]; for $\gamma T\ll 1$ we have $\Delta\omega\propto Q_a$, due to the fact that in this case the increase of the atom-cavity interaction time gives the main contribution.

Of particular interest is the behavior of the cavity pulling versus the pulse area θ shown in Fig. 11: a value $\theta=\theta_0$ exists

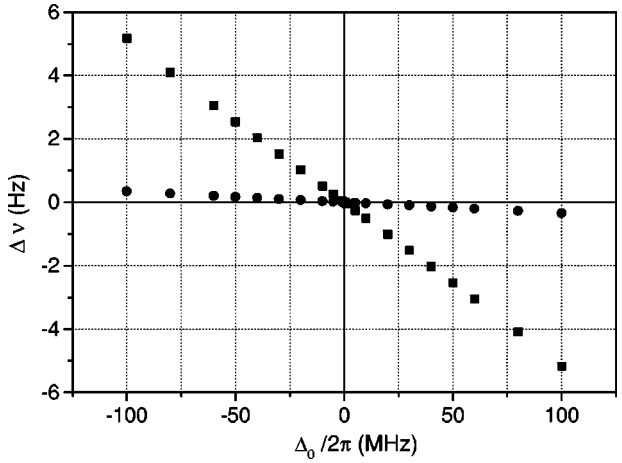

FIG. 8. Computed residual light shift versus the optical detuning Δ_0: $\Gamma_p=10\,000\ \mathrm{s}^{-1}$, $t_p=0.5$ ms, $\gamma_1=\gamma_2=200\ \mathrm{s}^{-1}$, $t_1=0.2$ ms, and $T=1$ ms. Circles: $b_e t_1=12\pi/25$. Squares: $b_e t_1=\pi/4$.

which cancels the effect. This value is given by the following relation easily obtained from Eq. (26):

$$\theta_0=\pi-\arccos\left(\tanh\left[\frac{k}{2\gamma}(1-e^{-\gamma T})\right]\right). \tag{27}$$

A value of θ_0 not far from $\pi/2$ may be a useful trade-off to minimize both the residual light shift and the cavity-pulling effect and this fixes the optimal operating range for k as can be seen from Fig. 9 and from Eq. (27). It is interesting to note that the elimination of the cavity-pulling effect, or at least its strong reduction, is made possible in the POP operation by the Ramsey interaction technique instead of the Rabi one typically used in cell frequency standards.

V. FREQUENCY STABILITY

We have seen in Sec. III that under suitable operating conditions the transfer of laser fluctuations to the output signal can be made unimportant, so that the short-term fre-

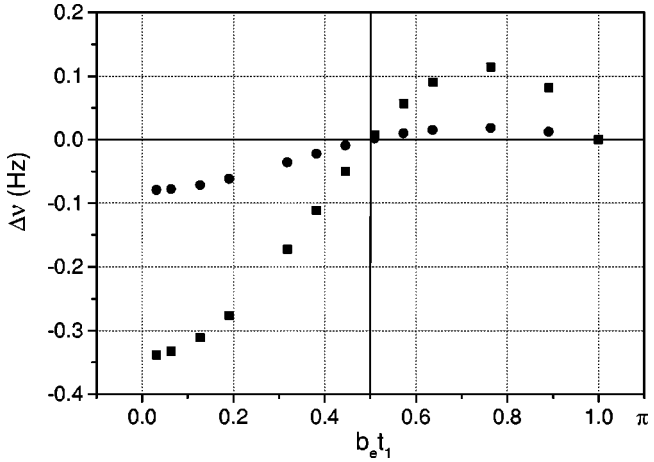

FIG. 9. Computed frequency shift versus the microwave pulse area for two different values of the pumping rate. Square: $\Gamma_p=5000\ \mathrm{s}^{-1}$. Circle: $\Gamma_p=10\,000\ \mathrm{s}^{-1}$. $\Delta_0/2\pi=1$ MHz.

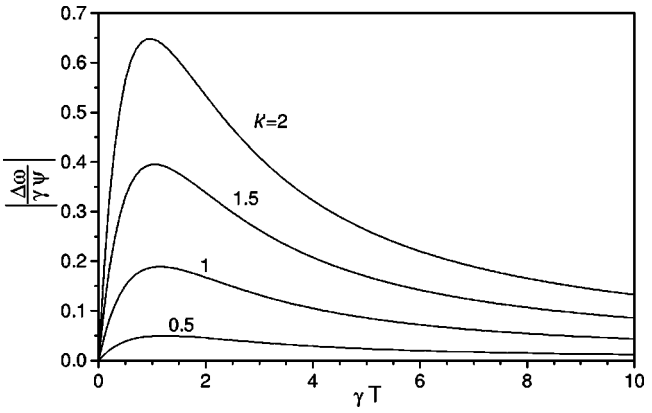

FIG. 10. Numerical evaluation of the cavity pulling as a function of γT: $\theta=\pi/2$, $\gamma_1=\gamma_2=\gamma$, and $k'=k/\gamma$.

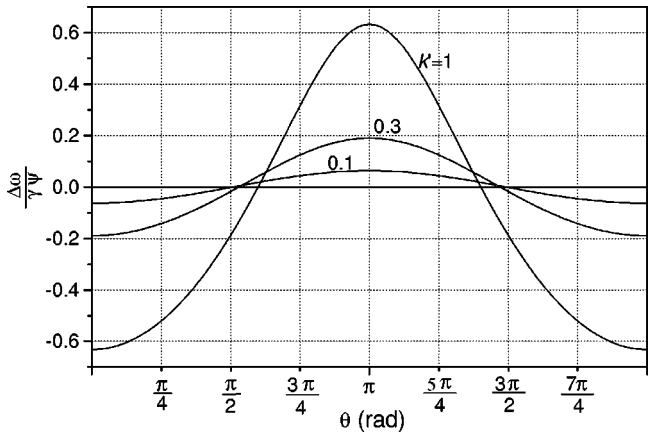

FIG. 11. Calculated cavity pulling versus the microwave pulse area: $\gamma T=1$.

quency stability of the POP standard is limited in principle only by the thermal detection noise and by the microwave synthesizer noise. As regards the medium term stability ($\tau>1000$ s), we have seen in Sec. IV that the cavity-pulling effect can be strongly reduced with a proper choice of θ, so that the main instability source is expected to be the temperature coefficient of the buffer gas, which may be reduced through a proper mixture of different buffer gases and with an adequate temperature control. It is then interesting to find now the theoretical stability limit due to the thermal detection noise. We assume an additive Gaussian noise at the output of the microwave cavity with white spectral power density $S_n(\omega)$ given by

$$S_n(\omega)=Fk_BT_0, \tag{28}$$

where F is a noise figure which accounts for the noise of the heterodyne receiver, k_B is the Boltzman constant, and T_0 the temperature of the detection system. The variance of the thermal noise sampled by the detection window is

$$\sigma_n^2=\int_{-\infty}^{+\infty}|H(\omega)|^2S_n(\omega)d\omega=\frac{2\pi}{t_d}Fk_BT_0, \tag{29}$$

where $H(\omega)=(\sin\omega t_d/2)/(\omega t_d/2)$ is the Fourier transform of the rectangular detection window.

We also assume that the error signal required to lock the microwave generator to the central Ramsey fringe is obtained through a square-wave modulation of period $T_m=2T_c$, applied to the generator itself. In this case the POP standard operation is very similar to that of an atomic fountain, but with a signal-to-noise ratio in the 1-Hz bandwidth given by $\sqrt{P_d/\sigma_n^2}$, where P_d is the power at the cavity output averaged over the detection window and σ_n^2 is given by Eq. (29). The frequency standard deviation can then be written as [14]

$$\sigma_y(\tau)=\frac{\sqrt{2\pi}}{Q_a}\sqrt{\frac{Fk_BT_0}{P_d}}\sqrt{\frac{T_c}{t_d}}\tau^{-1/2}, \tag{30}$$

where τ is the measurement time. To improve the frequency stability, Eq. (30) mainly requires one to maximize the product $Q_a\sqrt{P_dt_d/T_c}$; in typical operating conditions it may be easily found:

$$\max(Q_a\sqrt{P_dt_d/T_c})\Rightarrow\gamma T=0.7-0.8. \tag{31}$$

The condition (31) for maximum stability implies also maximum cavity-pulling shift (Fig. 8) so that it becomes mandatory to operate with $\theta\simeq\theta_0$ [Eq. (27)].

For a numerical estimation of the short-term stability foreseen by Eq. (30), we consider the case of ^{87}Rb operating at $T=60$ °C. For a cell of length $L=40$ mm and diameter $2R=40$ mm with 2000 Pa (15 Torr) of buffer gases (N_2 and Ar) we have $\gamma_1\sim\gamma_2=200$ s^{-1} and $\Gamma^*=1.9\times10^9$ s^{-1}. Considering the timing sequence $T\sim\gamma_2^{-1}=4$ ms, $t_d=4$ ms, $t_p=2$ ms, and $t_1=0.5$ ms we have $T_c=11$ ms and $Q_a=1.1\times10^8$. Moreover, with a cavity operating in the TE_{011} mode ($\eta'Q_L\sim4000$) the output power is $P_d=100$ pW. Equation (30) gives, for the above example,

$$\sigma_y(\tau)=2.8\times10^{-13}\tau^{-1/2}, \tag{32}$$

a stability limit not far from the typical performances of H-masers, at least in the short-term period.

Residual light shift and cavity pulling are expected not to impair the predicted short-term stability as will be shown in the next section on the basis of the experimental results.

VI. EXPERIMENTAL RESULTS

In this section we report the experimental Ramsey pattern observed in the free-induction decay signal at the end of the second microwave pulse, showing the expected doubling of the atomic quality factor. The residual light shift and cavity pulling will be also reported, showing the agreement of their behavior with theoretical predictions.

With reference to Fig. 1, we use an aluminum cavity operating in the TE_{011} mode and a quartz cell containing ^{87}Rb vapor (98%) and a mixture of buffer gases (Ar and N_2) at a total pressure of 3300 Pa (25 Torr). At the operating temperature $T_0=63$ °C for our cell (length $L=18$ mm, diameter $2R=32$ mm) we have $\Gamma^*=3\times10^9$ s^{-1}, $\gamma_1\sim\gamma_2\sim350$ s^{-1}, $n\sim4\times10^{11}$/cm^3, and $\zeta=4.5$. The loaded quality factor of the cav-

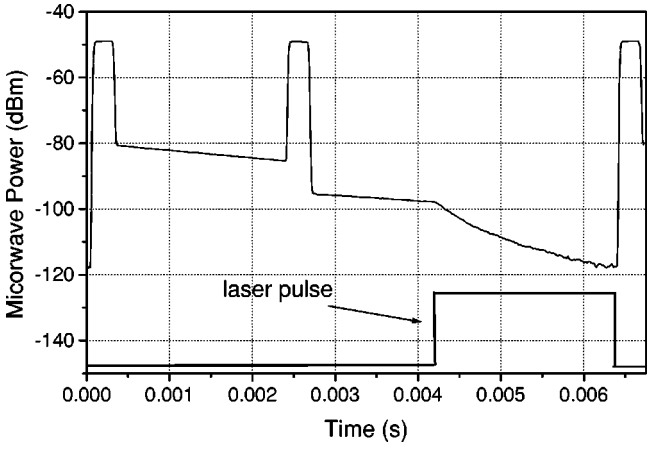

FIG. 12. Atomic coherence evolution observed at the cavity output versus time. The spectrum analyzer resolution bandwidth is 30 kHz, the video bandwidth is 30 kHz, and the center frequency is 6.834 686 670 GHz. The microwave detuning is $\Omega_\mu/2\pi=10$ Hz and $T=2.5$ ms. We superimposed in this figure the laser pulse to make more evident the coherence destruction.

ity is $Q_L=17\,000$ and the filling factor is $\eta'=0.4$.

The laser is tuned to the $|5\,^2S_{1/2},F=1\rangle \rightarrow |5\,^2P_{1/2},F=2\rangle$ D_1 optical transition of ^{87}Rb; it is linearly polarized and with the longitudinal quantization static magnetic field it excites the $\sigma^{\pm}$ transitions, performing a complete depletion of the $|5\,^2S_{1/2},F=1\rangle$ ground-state sublevel through optical pumping. Its power density at the cell entrance is 0.5 mW/cm^2, corresponding to a longitudinal pumping rate $\Gamma_p(0)=12\,000$ s^{-1}.

In the experiments we use $t_p=2$ ms, $t_1=200$ μs, and 2.5 ms$<T<$3.5 ms. The condition (10) requires $\Gamma_p(0) \gg 2000$ s^{-1} and is satisfied in our case.

The microwave power required to achieve $\pi/2$ pulses is of the order of 100 nW. The heterodyne detector is a spectrum analyzer operating in the video mode and synchronized to the timing pattern.

A typical cavity output signal is shown in Fig. 12; the free-induction decay ($\propto|\delta_{\mu\mu'}|^2$) is observed between the two Ramsey pulses and in the detection region between the second microwave pulse and the laser pulse. A reduction in this case of 20 dB of the microwave coherence may be also observed during the laser pulse and before a new cycle starts up.

The amplitude of the central Ramsey fringes observed at the end of the second microwave pulse is shown in Fig. 13 versus the detuning $\Omega_\mu/2\pi$ for $\theta=\pi/8$ and $\theta=\pi/2$. The theoretical predictions of Figs. 4 and 5 are clearly confirmed by the experimental curves; the fringe linewidths fully agree with relations (20) and, in the case of $\pi/2$ pulses, the observed quality factor is $Q_a=1\times10^8$. The frequency shift between the two curves is mainly due to the residual light shift in the lower curve, $\theta=\pi/8$ being very far from the optimal value, as found in Sec. III.

The output power at the end of the second pulse is $P_d=1$ pW and the signal-to-noise ratio is $R_{S/N}=10^4$ in the 1-Hz bandwidth. An increase of 20 dB in P_d, corresponding to an increase of an order of magnitude of $R_{S/N}$, is expected for a cell with optimized geometrical dimensions, allowing us to reach the stability limit reported in Eq. (32).

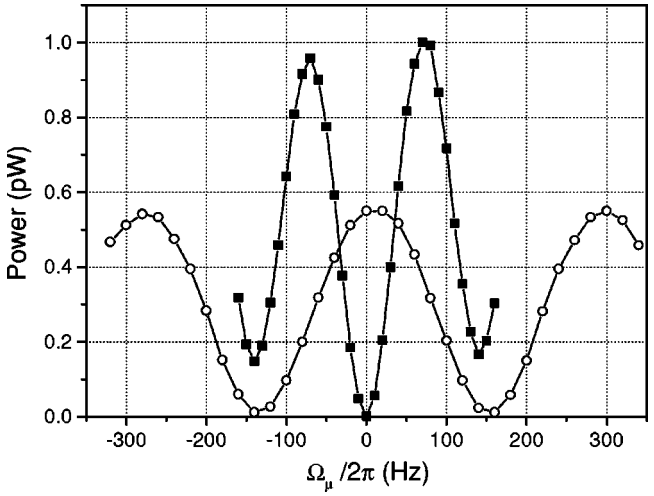

FIG. 13. Ramsey fringes observed in the free-induction decay signal. Squares: $\theta=\pi/2$. Circles: $\theta=\pi/8$. $T=3.5$ ms.

Ramsey fringes have also been observed in the transmitted optical signal; in this case no doubling of the quality factor is present and the linewidth is given by the well-known relation $\Delta\nu_{1/2}=1/2T$ [15].

To measure the residual light shift we lock the laser frequency to the D_1 line through the saturated absorption signal observed in an external cell containing ^{87}Rb and then we lock the synthesizer quartz frequency (10 MHz) to the central Ramsey fringe detected via the transmitted optical signal.

In Fig. 14 we report the measured frequency shift of the clock transition due to a laser frequency change of 10 MHz as a function of laser intensity for different values of θ (the fine-tuning of the laser is performed by an acousto-optic modulator).

The experimental data show that (i) the light shift decreases when the laser intensity increases due to the higher rate of coherence destruction and (ii) a value of θ exists

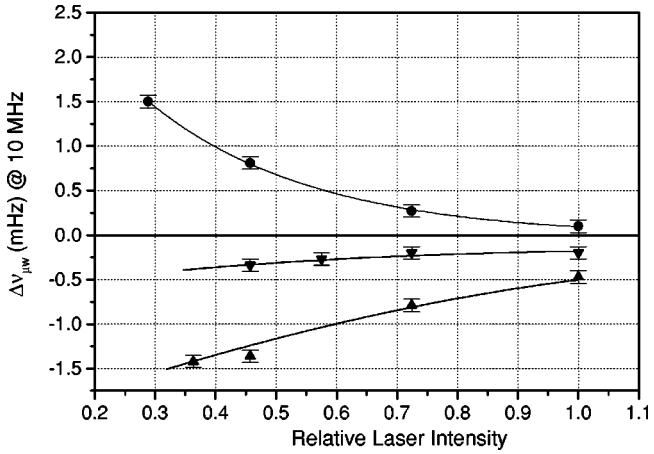

FIG. 14. Differential frequency shift of the POP versus the laser intensity for different values of θ. Circles: $\theta=0.8\pi/2$. Down triangles: $\theta=0.63\pi/2$. Up triangles: $\theta=0.5\pi/2$. The maximum laser intensity is 0.5 mW/cm^2. $T=3.5$ ms.

which significantly reduces the light-shift contribution at any laser intensity.

The experimental optimum value turns out $\theta_{expt}=0.7\pi/2$ lower than the theoretical value $\theta_{th}=\pi/2$; this difference is due to the spatial distribution of the TE_{011} mode inside the cavity: the real microwave field coupled to the atoms depends on their position inside the cell, whereas in the theoretical analysis the microwave Rabi frequency has been assumed position independent.

Anyway, with a laser intensity of 0.7 mW/cm^2 and a microwave power corresponding to $\theta=0.7\pi/2$ we have measured the relative variation of the POP frequency versus the laser frequency deviation to be $(1.6\pm0.5)\times10^{-13}$/MHz. This value is lower by at least three orders of magnitude when compared to the case of the traditional approach [4].

In the same experimental setup we have also measured the cavity-pulling shift; in our case the gain factor is $k=450\ s^{-1}$. In Fig. 15 we report the measured frequency shift versus θ for three different values of the cavity detuning parameter ψ. Around $\theta_0\simeq0.9\pi/2$ the output frequency hardly depends on the cavity detuning as expected from the theoretical computations. In the experimental conditions ($k/\gamma\simeq1.3$ and $\gamma T\simeq0.7$) Eq. (27) yields $\theta_0=1.2\pi/2$, higher than the experimental value for the same reasons already discussed in the case of the light shift. The preliminary results reported in this section prove the theoretical predictions: the possibility of (a) doubling the atomic quality factor, (b) reducing by several orders of magnitude the light shift, and (c) eliminating the cavity pulling. In particular the residual light-shift effect may be further reduced, increasing the laser intensity by a factor of 2 or 3 and with a proper stabilization of the laser frequency so that the short-term stability limit reported in Eq. (32) may practically be achieved.

VII. CONCLUSIONS

We have examined in this paper the scheme of pulsed optical pumping applied to gas cell frequency standards. Under suitable operating conditions the system approaches the two-level scheme; moreover, the detection of the free-induced decay signal, instead of the more common optical transmission one, together with a Ramsey-type interaction to observe the hyperfine transition, lead to the following advantages: (a) no laser background signal is present in the atomic response, (b) the atomic line quality factor is increased by a factor of 2 with respect to the traditional approaches, (c) the light-shift effect may be canceled, and (d) the cavity-pulling effect may be strongly reduced. The resulting short-term frequency stability is limited by the system thermal noise only, while the medium-term frequency stability is limited by the buffer-gas temperature coefficient. The preliminary experimental results reported in Sec. VI confirm the main theoretical expectations. These features make then the POP frequency standard extremely attractive, especially in those fields where a simple and reliable implementation is required, such as space applications.

APPENDIX

We are looking for the general solutions of the system (16). The initial conditions are given by the Bloch vector at the end of the first microwave pulse ($t=0^+$); when Eq. (10) is satisfied and neglecting the Rabi pedestal, we have, from Eq. (14),

$$\delta_{\mu\mu'}(0^+)=-\frac{1}{2}\sin\theta,$$

$$\Delta(0^+)=\cos\theta. \tag{A1}$$

It is usual at this point to write the hyperfine coherence in the form

$$\delta_{\mu\mu'}(t)=M(t)e^{i\varphi(t)},\quad t>0. \tag{A2}$$

System (16) becomes

$$\dot{\Delta}(t)+\gamma_1\Delta(t)=-4kM^2(t),$$

$$\dot{M}(t)+\gamma_2M(t)=kM(t)\Delta(T),$$

$$\dot{\varphi}(t)+\Omega_\mu=k\psi\Delta(t), \tag{A3}$$

and the initial conditions (A1) become

$$\Delta(0)=\cos\theta,$$

$$M(0)=\frac{1}{2}|\sin\theta|,$$

$$\varphi(0)=\begin{cases}\pi & \text{when}\quad \sin\theta>0,\\ 0 & \text{when}\quad \sin\theta<0.\end{cases} \tag{A4}$$

The first two differential equations of Eqs. (A3) are coupled while the third one can be directly integrated as follows:

$$\varphi(t)=\varphi(0)-\Omega_\mu t+k\psi\int_0^t\Delta(t')dt', \tag{A5}$$

which clearly shows the time-dependent contribution of the cavity detuning to the phase evolution of the coherence (cav-

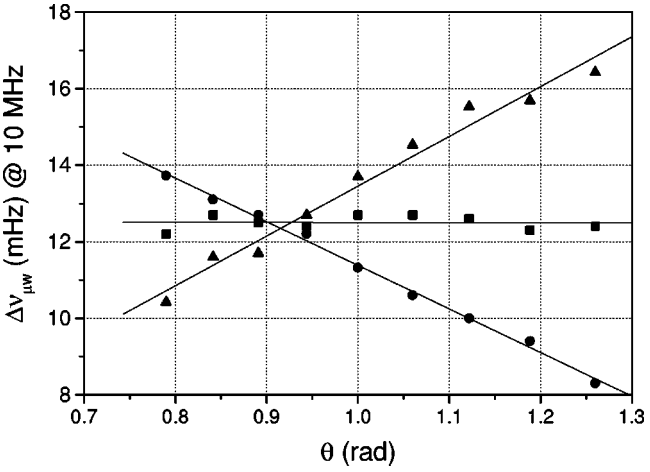

FIG. 15. Cavity pulling versus the microwave pulse area θ in units of $\pi/2$. Triangles: $\psi=+0.69$. Squares: $\psi=-0.05$. Circles: $\psi=-0.69$. $T=3.5$ ms.

ity pulling). Analytical solutions for $\Delta(t)$ and $M(t)$ with initial conditions (A4) are found, when $\gamma_1=\gamma_2=\gamma$, with the aid of the substitution $M(t)=Ae^{-\gamma t}\mathrm{sech}[y(t)]$; their expressions are

$$\Delta(t) = -e^{-\gamma t}\tanh\left[\frac{k}{\gamma}(1-e^{-\gamma t}) - \tanh^{-1}\cos\theta\right],$$

$$M(t) = \frac{1}{2}e^{-\gamma t}\mathrm{sech}\left[\frac{k}{\gamma}(1-e^{-\gamma t}) - \tanh^{-1}\cos\theta\right]. \quad \text{(A6)}$$

Inserting the first of Eqs. (A6) in Eq. (A5) we have

$$\varphi(t) = \varphi(0) - \Omega_\mu t - \psi\ln\left\{|\sin\theta|\cosh\left[\frac{k}{\gamma}(1-e^{-\gamma t}) - \tanh^{-1}\cos\theta\right]\right\}. \quad \text{(A7)}$$

At the end of the decay time $t=T$ the frequency shift due to the cavity pulling is from Eq. (A7):

$$\Delta\omega = -\frac{\psi}{T}\ln\left\{|\sin\theta|\cosh\left[\frac{k}{\gamma}(1-e^{-\gamma T}) - \tanh^{-1}\cos\theta\right]\right\}, \quad \text{(A8)}$$

which is equivalent to Eq. (26).

[1] G. Mileti *et al.*, IEEE J. Quantum Electron. **34**, 233 (1998); J. Kitching *et al.*, IEEE Trans. Instrum. Meas. **49**, 1313 (2000); M. Zhu, in *Proceedings of Joint Meeting 17th European Frequency and Time Forum and 2003 IEEE International Frequency Control Symposium, Tampa, FL, 2003*, edited by J. Vig (IEEE, New York, 2003).

[2] C. O. Alley, in *Quantum Electronics*, edited by C. H. Townes (Columbia University Press, New York, 1960).

[3] M. Arditi and T. R. Carver, IEEE Trans. Instrum. Meas. **13**, 146 (1964).

[4] J. Vanier and C. Audoin, *The Quantum Physics of Atomic Frequency Standards* (Adam-Hilger, Bristol, England, 1989).

[5] J. C. Camparo and J. C. Coffer, Phys. Rev. A **59**, 728 (1999).

[6] N. Cyr, M. Tetu, and M. Breton, IEEE Trans. Instrum. Meas. **42**, 640 (1993).

[7] J. Vanier, A. Godone, and F. Levi, Phys. Rev. A **58**, 2345 (1998).

[8] A. Godone, F. Levi, and S. Micalizio, Phys. Rev. A **65**, 033802 (2002).

[9] F. Levi, A. Godone, and J. Vanier, IEEE Trans. Instrum. Meas. **47**, 466 (2000); M. Zhu and L. S. Cutler, in *Proceedings of the 32nd Precision Time and Time Interval (PTTI) Systems and Applications Meeting, Roston, Virginia, 2000*, edited by L. Breakiron (USNO, Washington, 2001); C. Affolderbach, G. Mileti, C. Andreeva, T. Karaulanov, and S. Cartaleva, in *Proceedings of Joint Meeting 17th European Frequency and Time Forum and 2003 IEEE International Frequency Control Symposium, Tampa, FL, 2003* (Ref. [1]), pp. 27–30.

[10] T. C. English, E. Jechart, and T. M. Kwon, in *Proceedings of the 10th Precision Time and Time Interval (PTTI) Applications and Planning Meeting, Washington, 1978*, edited by L. J. Rueger (NASA, Maryland, 1979); F. Levi, C. Novero, A. Godone, and G. Brida, IEEE Trans. Instrum. Meas. **46**, 126 (1997).

[11] E. I. Alekseyev, Y. N. Bazarov, and G. I. Telegin, Radio Eng. Electron. Phys. **20**, 73 (1975); E. I. Alekseyev, Y. N. Bazarov, and A. E. Levishin, *ibid.* **19**, 77 (1974).

[12] A. Godone, F. Levi, and S. Micalizio, *Coherent Population Trapping Maser* (CLUT Editrice, Torino, Italy, 2002).

[13] L. Allen and J. H. Eberly, *Optical Resonance and Two-Level Atoms* (Dover, New York, 1987); M. Sargent III, M. O. Scully, and W. E. Lamb, Jr., *Laser Physics* (Addison-Wesley, Reading, MA, 1974).

[14] G. Santarelli *et al.*, Phys. Rev. Lett. **82**, 4619 (1999).

[15] N. Ramsey, *Molecular Beams* (Clarendon Press, Oxford, 1956).